

Hydrogen evolution and defect creation in amorphous Si:H alloys

D. K. Biegelsen, R. A. Street, C. C. Tsai, and J. C. Knights

Xerox Palo Alto Research Center, 3333 Coyote Hill Road, Palo Alto, California 94304

(Received 23 June 1979)

Changes in the composition and electronic properties of plasma-deposited *a*-Si:H after annealing at temperatures through 600° C are studied by ESR, luminescence, infrared spectroscopy and hydrogen evolution. The generation of paramagnetic defects in *a*-Si:H on annealing is found to depend only on the amount of hydrogen evolved. The relation of peaks in the hydrogen-evolution rate to specific local hydrogen-bonding environments is studied and shown to be dominated by the effects of diffusion and sample microstructure.

I. INTRODUCTION

It is well known that hydrogen incorporation in amorphous and damaged crystalline silicon generally decreases the density of states in the gap. Conversely, it has been shown that removing hydrogen (among other changes) increase the density of gap states, increases the paramagnetic spin density,¹ and quenches the band-edge luminescence.² In glow discharge deposited *a*-Si:H (and, to varying degrees, in all forms of hydrogenated amorphous silicon), the hydrogen is bonded in various configurations depending on the specific deposition conditions. The occurrence of the dominant configurations, $\equiv\text{SiH}$, $\equiv\text{SiH}_2$, $-\text{SiH}_3$, and $(\text{SiH}_2)_n$ (or polysilane chainlike regions), has been correlated on the one hand with the deposition parameters,³ and on the other with the presence of traps and nonradiative recombination centers.⁴ Annealing studies have been useful in characterizing the role of hydrogen in *a*-Si:H, particularly because a great range in conditions can be obtained systematically in a single sample. The prevailing notion in the literature,⁵⁻⁷ although contradictory evidence exists,⁸ is that upon annealing, first a peak in the hydrogen-evolution rate occurs at $T_A \sim 320^\circ\text{C}$, corresponding to a local release of one kind of bound H, e.g., H_2 from $\equiv\text{SiH}_2$ sites, followed by a second and final peak at $\sim 600^\circ\text{C}$, corresponding to release of atomic H. It has been assumed that effects due to diffusion can be neglected.

The existence of microstructure (i.e., columnar growth having a characteristic diameter ~ 100 – 200 Å) has recently been observed and found to be dependent upon the deposition conditions.⁹ This inhomogeneous morphology should affect the specific hydrogen incorporation and evolution. Furthermore, evidence from secondary ion mass spectroscopy (SIMS) measurements indicates that hydrogen diffusion is activated with an energy ~ 1.5 eV, which depends on the hydrogen content of the sample.¹⁰ It was the purpose of this study, therefore, to carry out simultaneous mea-

surements of luminescence, electron spin resonance, infrared, and hydrogen-evolution spectra on a set of samples spanning the range of deposition parameters and consequent range of as-deposited internal structures. From the results we hoped to obtain detailed information about the specific hydrogen-bonding configurations and the kinetics of release from the samples, and further, to see if the correlations between the distribution of hydrogen configurations and gap states found for as-deposited materials held also for materials after progressive stages of H evolution. Section II contains a brief description of the experimental methods and results. In Sec. III we discuss the results, and we present our conclusions in Sec. IV.

II. EXPERIMENT

Batches of eight to ten samples of undoped *a*-Si:H were plasma deposited from SiH_4 -Ar onto roughened Corning 7059 glass substrates. Gas concentration (volume percentage of SiH_4 in mixture) ranged from 5 to 100%; substrate temperatures ranged from 25 °C (RT) to 230 °C; power absorbed in the plasma was varied from 1 to 25 W; dc bias depended on rf power and sample placement on anode or cathode. (For details, see Ref. 4.) We include the deposition parameters of the batches in Table I. Unless noted, all samples were approximately 5 μm thick. The individual samples of each batch were isochronally annealed at the various temperatures T_A in an initial pressure of 100 mTorr dry N_2 for ten minutes. Evolved hydrogen was monitored manometrically. A single sample of each batch was annealed at constant heating rate of 20 °C/min to obtain continuous differential gas evolution curves. Total pressures of the order of one Torr were generated in a constant volume of ~ 50 cm³. After annealing, the ESR and luminescence spectra of each sample were measured. (For details, see Ref. 4.) Infrared measurements were run on a sample codeposited on a roughened crystalline-silicon substrate and sequentially annealed.

TABLE I. Sample properties. (Hydrogen environments are listed in order of relative abundance.)

Symbol	Deposition conditions	H environments	Microstructure
△	100%; 1 W; RT; anode	(SiH ₂) _n , ≡SiH	
▲	100%; 1 W; RT; cathode	(SiH ₂) _n , ≡SiH	
○	100%; 1 W; 230°C; anode	≡SiH	
●	5%; 20 W; 150°C; anode	(SiH ₂) _n , =SiH ₂	*
□	5%; 25 W; RT; anode	(SiH ₂) _n , =SiH ₂	*
■	5%; 25 W; RT; cathode	=SiH ₂ , ≡SiH, (SiH ₂) _n	

Figure 1(a) shows the variation of the ESR spin density N_s with annealing temperature T_A . The initial spin density in all samples studied is seen to decrease with an approximate activation energy of 0.5 eV reaching a minimum between 200 and 300 °C. With further increase in T_A , N_s increases in significantly different ways for samples with different deposition conditions. For example, only the anode samples deposited at 5% concentration and ~25 W power show a large increase around 300 °C. Similarly, other sample-dependent structures can be seen around 400 °C and above 500 °C. The ESR lines occur at $g \sim 2.0055 \pm 0.0002$ (except for the 100%; 1W anode samples between approximately 300 and 400 °C for which $g \sim 2.0045$.) The peak-peak line width of ~7.5 G narrows at high spin densities (occurring both at low and high temperatures) in agreement with earlier findings.¹¹ A final experimental result we note here is that the 5% and 25 W samples (both anode and cathode) in the range 200–400 °C show an increase of N_s by a factor ~2 with time ($\tau \sim 1$ d) after annealing in the range 200–400 °C. (For clarity we show the data long after annealing only for the 150 °C sample.) The 100% and 1 W samples show no observable changes with time.

The photoluminescence is a broad, featureless, Stokes-shifted band. In Fig. 1(b) we show the luminescence efficiency data on the same samples as in Fig. 1(a) (measured several days after annealing). The similarity in structure in (the reciprocal of) the luminescence and the spin density is striking. Figure 1(c) shows the annealing dependence of the energy of the luminescence peak. Again the gross features above ~250 °C correlate, maximum shifts occurring along with maximum changes in I_L and N_s . From the detailed similarity in the changes with annealing temperature, we are led to the conclusion that, irrespective of the microscopic origin of defects at low and high temperatures, an increase in spin density leads to a decrease in intensity and energy of the luminescence. In contrast, Fig. 1(d) shows that the variation of luminescence linewidth full width at half maximum (FWHM) with annealing temperature is different for

the low- and high-temperature regimes. The width generally decreases from ~0.45 to ~0.3 eV by ~300 °C (i.e., where N_s is a minimum) and then stays approximately constant.

We turn now to the hydrogen evolution during annealing. Figure 2(a) shows the increase in hydrogen evolved (normalized to sample volumes) as a function of temperature. Figure 2(b) contains the derivative spectra of representative curves (plotted logarithmically) to show more clearly the structure. Isochronal anneal data are essentially the same as the constant-heating-rate data with a slight shift to lower temperatures (~20 °C). The abrupt changes above 650 °C are due to H release on sample crystallization (cf. Ref. 8).

Figure 2(b) demonstrates vividly that one cannot describe the hydrogen evolution simply in terms of two characteristic peaks. The peak positions vary with deposition conditions. In spite of this variability, it can be seen that the peaks correspond very closely to the regions of rapid change (Fig. 1) in the luminescence and spin density.

Earlier publications have associated infrared bands with silicon-hydrogen bonding configurations.³ Changes in the ir spectra on annealing have been published by the University of Chicago group (cf. Ref. 8). Our results are in close agreement with their findings. Figure 3 contains the variation with T_A of the ir absorbance at various wavelengths for a representative sample (100%; 1 W; 30 °C anode). The 840 cm⁻¹ mode, which arises only from (SiH₂)_n, is seen to disappear by ~400 °C; thus, the change above 400 °C in the absorption remaining in the 2090 cm⁻¹ band [arising from =SiH₂ and/or (SiH₂)_n] must represent =SiH₂ evolution. Comparison with the corresponding evolution spectrum in Fig. 2 demonstrates that the 320 °C peak is dominated by the decrease of the (SiH₂)_n-related ir absorption and that ≡SiH and =SiH₂ evolve over a broad temperature range with a rate peaking near 600 °C. Figure 4 contains results for a set of (5%; 25 W anode) samples deposited at various substrate temperatures; all have strong columnar growth patterns. The only peaks observable in these samples occur at 330 and 430 °C and are plotted

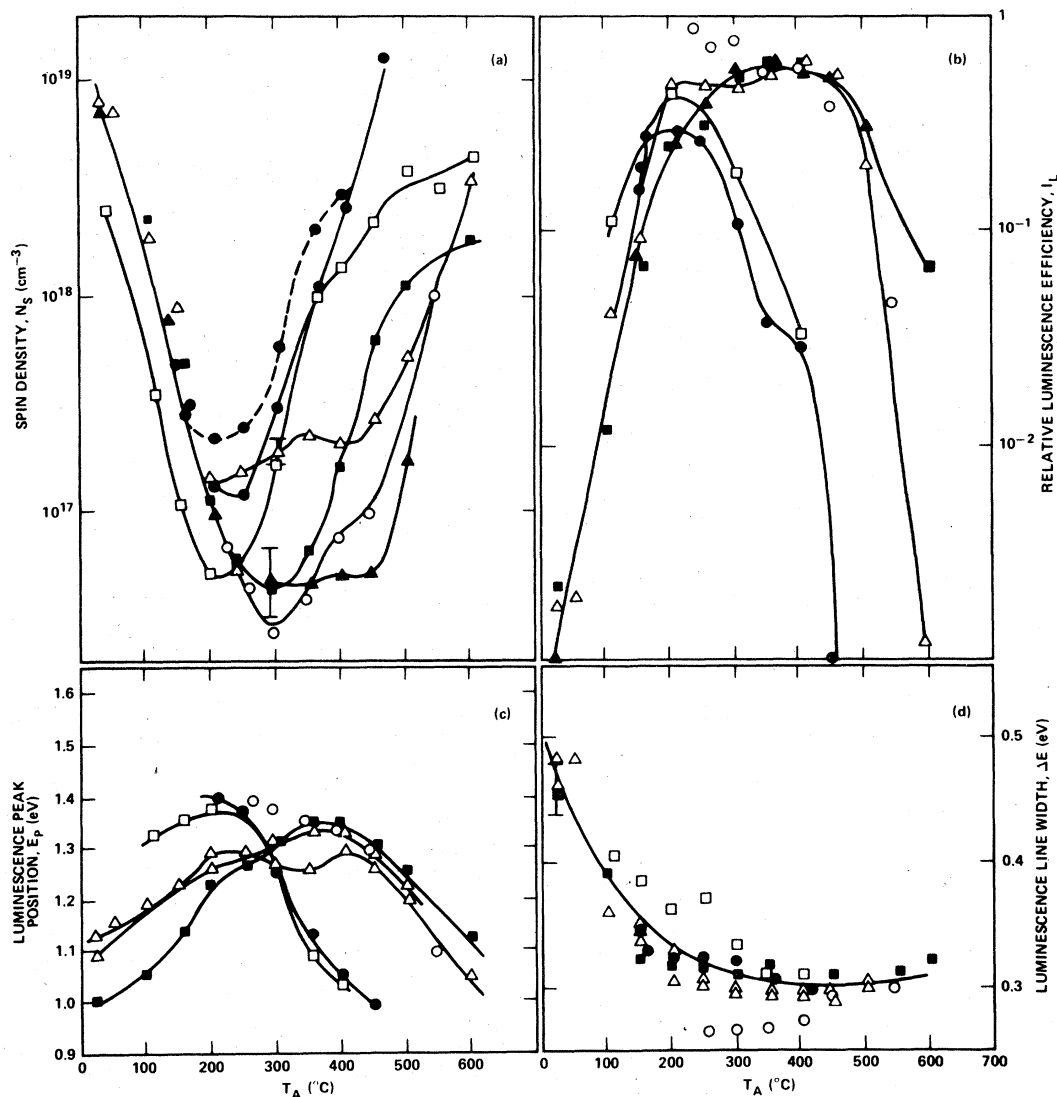


FIG. 1. (a) Spin density versus annealing temperature T_A . Dash line shows asymptotic value of 5%; 20 W sample. (b) Luminescence intensity versus T_A . (c) Luminescence peak energy versus T_A . (d) Luminescence bandwidth (full width at half maximum) versus T_A .

as circles and triangles, respectively. The lines represent the as-deposited (unannealed) ir-mode absorption constants for the same samples. [In these samples it has been argued that the dihydride modes arise predominantly from $(\text{SiH}_2)_n$ configurations.] The similarity between the sets of data implies a correspondence for these samples between the initial amount of $(\text{SiH}_2)_n$ and the amount of H released in the 330°C peak, and, unlike the samples of Fig. 3, between $\equiv\text{SiH}$ present and the 430°C release. This and other similar data lead us to conclude that the 430 and 600°C peaks are not uniquely associated with either $\equiv\text{SiH}$ or $=\text{SiH}_2$.

The association of the peak near 320°C with

$(\text{SiH}_2)_n$ does not hold in one of the samples studied here. Cathode samples prepared at 5%, 25 W and RT show almost no $(\text{SiH}_2)_n$ in the infrared. The $=\text{SiH}_2$ modes remain constant to above 400°C, whereas the $\equiv\text{SiH}$ mode (2000 cm^{-1}) drops off near 350°C with a temperature dependence very similar to that shown in Fig. 3. The derivative of the evolution curve in Fig. 2(a) shows a peak near 350°C corresponding to the $\equiv\text{SiH}$ decrease.

Diffusion, for hydrogen release from bulk sites, plays an important role in determining the temperature of the peak near 600°C (as opposed to the 320 and 420°C peaks). An example of this can be seen in Fig. 5 in which the evolution for (100%;

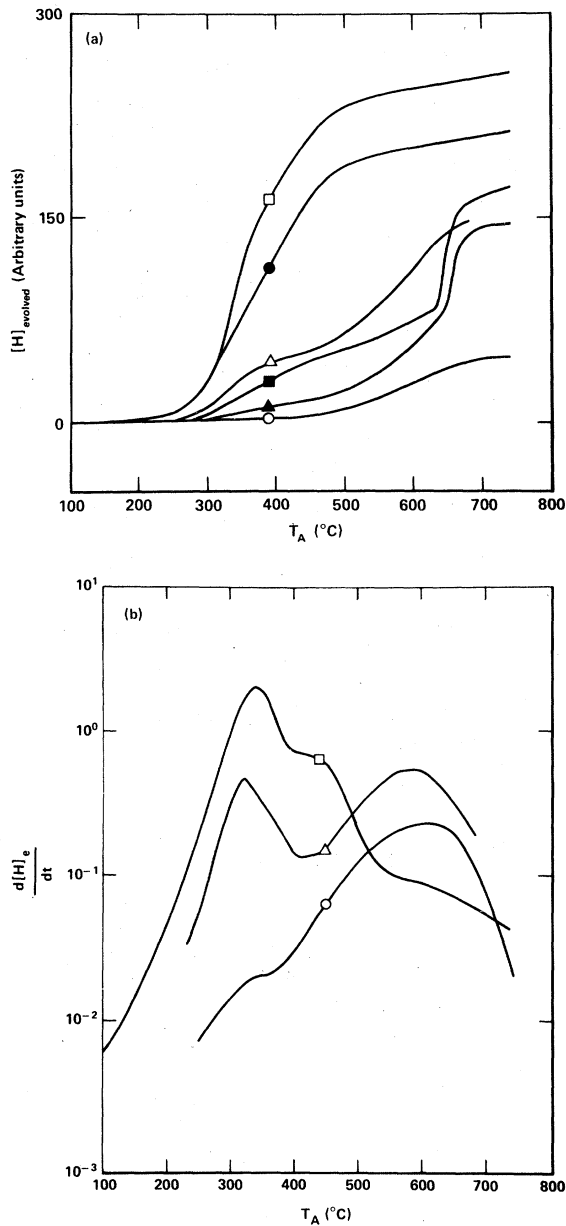


FIG. 2. (a) Hydrogen evolved (normalized to sample volume) for 20°C/min linear temperature ramp. (b) Derivative evolution spectra plotted logarithmically.

1 W, 230 °C; anode) samples having apparently homogeneous morphology are shown for two thicknesses. The relatively lower H release at low temperatures and the greater release upon crystallization in the thick sample is consistent with a diffusive delay.

Finally, before discussing the experimental results, we note that there is evidence from the infrared absorption and luminescence measurements for a post-anneal increase with time of bonded ox-

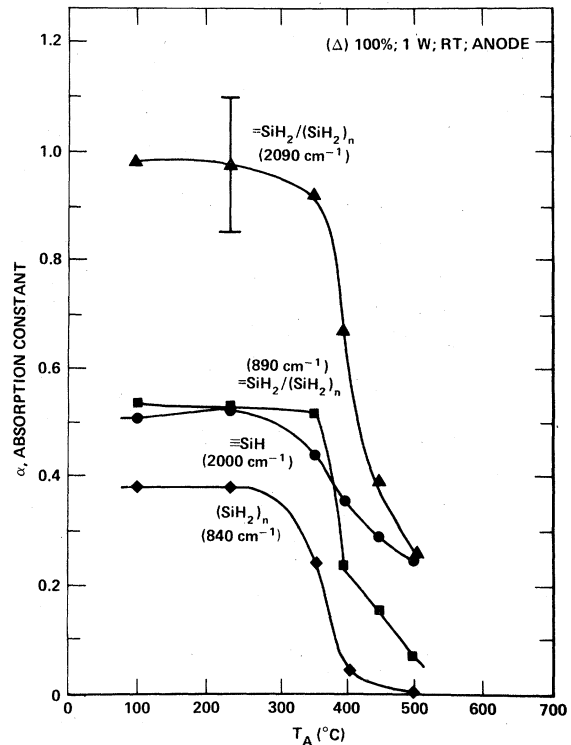


FIG. 3. Infrared absorption strengths versus T_A for the 100%, 1 W, RT, anode sample. The error bar is an estimate of the absolute error. Relative errors are of the order of the point size.

xygen. The ir indicates the growth of an oxygen band after the 320 °C polysilane evolution but shows no oxygen buildup otherwise. Luminescence seems to show a weak peak ~ 0.3 eV below the band edge luminescence which occurs apparently in all samples after anneals above ~ 500 °C. The temperature dependence of the low-energy peak is similar to that of the additional peak in samples intentionally doped with oxygen.⁴ The oxygenation seems to occur after hydrogen release and is least for samples with the least initial hydrogen concentration.

III. DISCUSSION

In an earlier article it has been shown that for a-Si:H samples, grown under a wide range of deposition conditions, a universal relation exists between the luminescence efficiency and spin density.⁴ This was explained by assuming a random distribution of photoexcited electrons and holes and a random distribution of nonradiative recombination centers.¹² These centers were in turn shown to be associated (within a factor of order unity) with an unpaired electron spin.⁴ In Fig. 6 we show

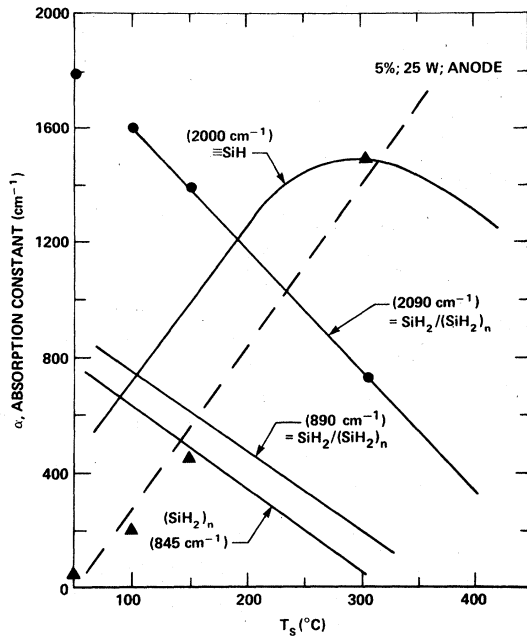


FIG. 4. Infrared mode strengths for samples deposited at T_s (solid lines); circles and triangles represent heights of 320 and 420°C peaks, respectively, for samples deposited at T_s . Relative scales for evolution data are arbitrary.

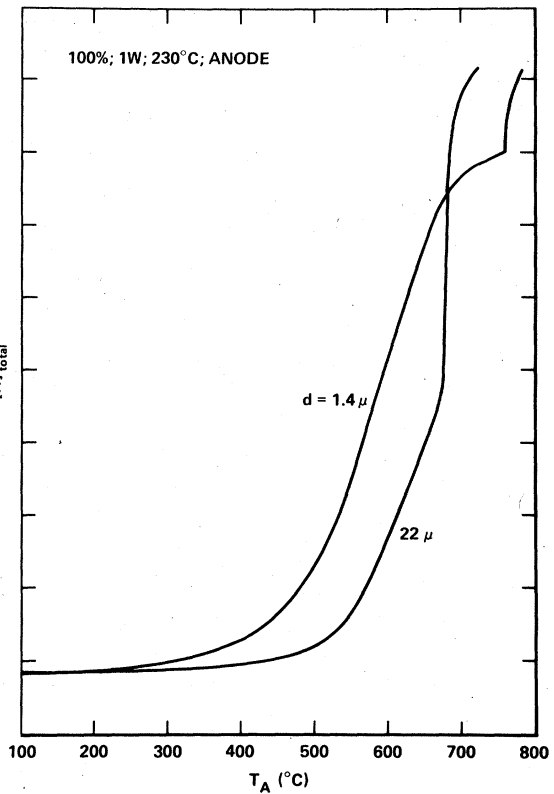


FIG. 5. Hydrogen evolution normalized to total hydrogen for identical samples of different thickness.

the two theoretical curves which bound the earlier data. (Note that this plot is shifted to higher spin density by a factor of 2.1, due to a saturation correction overlooked in the original paper. This shift does not change the conclusions.) The data from this work for annealed samples are shown in comparison to the previous as-deposited results. We observe that the same overall trend persists. The nonradiative quenching process therefore is most likely the same for defects created in removing hydrogen as well as for those existing initially; and further, the effectiveness as nonradiative recombination centers seems to be independent of the specific hydrogen configuration before evolution.

We note in passing that in work on electron- and helium-ion-bombarded a-Si:H (Ref. 13) similar annealing curves were observed for the spin density. The initial decrease in N_s reported here is in quantitative agreement with the annealing of point defects created by electron bombardment. Furthermore, a peak structure in $N_s(T_A)$ was observed in the vicinity of 400 °C and depended strongly on sample deposition conditions. A similar behavior is possibly indicated in Fig. 1(a) for the (100%; 1 W; RT; anode) samples (open triangles).

The dependence of the paramagnetic defect cre-

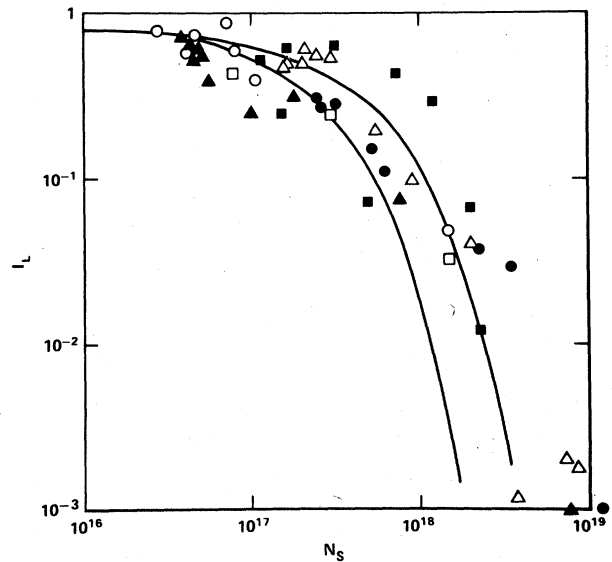


FIG. 6. Luminescence intensity plotted versus spin density. Solid lines span data for as-deposited samples (Ref. 4).

ation simply on the amount of hydrogen evolution and its independence of the initial local hydrogen environment is underlined by the results as plotted in Fig. 7. Here we have plotted $\log(N_s)$ versus the percentage of hydrogen evolved for each sample. We should draw attention here to the fact that isolated, relaxed Si-H bonds are in fact very strong and in the simplest picture should not re-release hydrogen at such low temperatures. A compensating energy-gain mechanism must be present. The exponential relation of Fig. 7 most likely arises from the fact that the hydrogen, which is first to evolve, does so because the remaining atoms can reconstruct (leaving very few spins per hydrogen released). Thus, the binding energy could be small due to a sterically restricted topology. The possibility for two H atoms leaving in a coordinated way, regaining the energy of molecule formation, has also been suggested.¹⁴ This most likely is also compatible with bond reconstruction. On the other hand, the most strongly bonded hydrogen would leave with less tendency for subsequent reconstruction. One might expect the final evolution to leave approximately one spin (dangling bond) per released hydrogen. However, because the mobility of defects is increasing with temperature, agglomeration of point defects and paired release of H_2 reduces the differential spin increase from 10^{-2} to 10^{-3} times the hydrogen evolution. This possibly accounts for the apparent saturation at high $[H]_{evol}/[H]_{total}$.

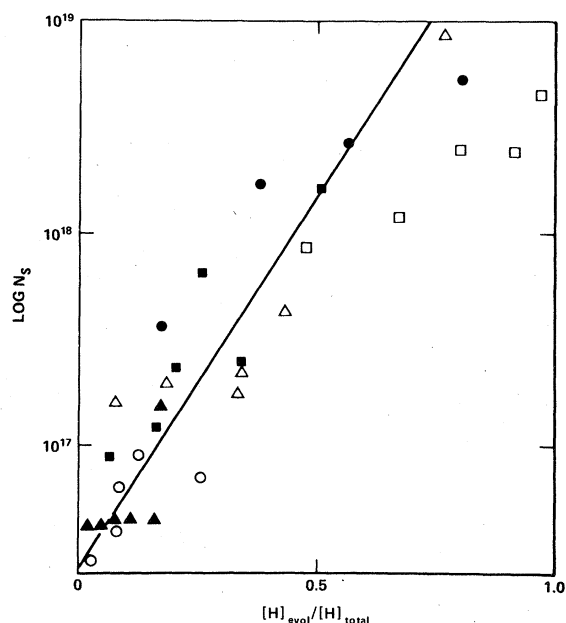


FIG. 7. $\log(N_s)$ versus percentage of hydrogen evolved.

We turn now to a discussion of the relation between the local hydrogen bonding configurations and the evolution kinetics. One expects the energy for H release at $=SiH_2$ sites to be different from that at $=SiH$ sites. Intuitively, we therefore might expect structure in the evolution to correspond simply to the local bonding configurations. The literature contains several reports of H evolution (BFZL,⁶ MMB,^{15(a)} TF,⁸ and MP⁷). The spectra differ greatly, but collectively the reported structures fall roughly into groups around 300 °C, 400 °C, and 500–650 °C. The structures have been ascribed to release from various specific local environments. In Fig. 8 we show a set of spectra which makes readily apparent the importance of sample characteristics other than local bonding configurations. The samples, all grown under nominally identical conditions (5%; 1W; 230 °C; anode) vary in thickness from 0.1 to 21 μm . These samples lie on the parameter space boundary between regions of columnar morphology and homogeneous growth.⁹ Since the columns have $\sim 100 \text{ \AA}$ diameter, we expect comparable amounts of isolated SiH/SiH₂ bonding to occur in bulk and "surface" regions. Thick samples show, in fact, the coexistence of peaks near 450 °C and 600 °C (unlike samples lying well into the columnar morphology region of the parameter space, for which no 600 °C peak is observed). The sudden increase in

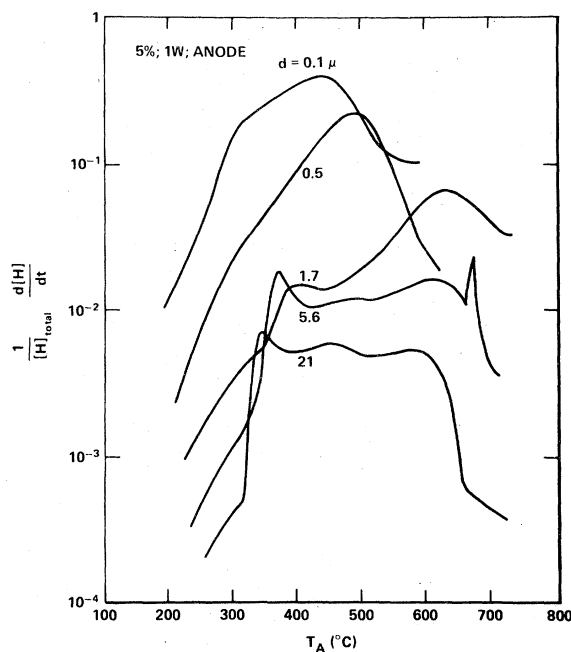


FIG. 8. Derivative evolution spectra normalized to total hydrogen evolved for samples of varying thickness. All samples have columnar morphology. Curves are offset by factors of e^{-1} .

(SiH₂)_n evolution near 350 °C, due to sample disintegration, leads us to conclude that the intercolumnar regions are filled with polysilanelike material. The post-anneal oxidation and increase in spin density corroborate the notion of a diphasic, columnar material. The shift to lower temperatures of the "600 °C" peak and the reemergence of the 420 °C peak after disintegration are explainable in terms of site location in the remnant columns. Below ~1 μm, no disintegration is evident and the "600 °C" peak shifts down toward 400 °C. All these spectra can be explained by assuming that the 400 °C peak corresponds to SiH/SiH₂ bonded on or very near to a surface, whereas the peak structure occurring for varying thicknesses from ~450 °C to above 650 °C (limited by crystallization—cf. Fig. 5) correspond to bulk SiH/SiH₂. The peak shift is determined by diffusion.

Summarizing our results we find: (1) In samples containing polysilane the 320 °C peak corresponds to hydrogen release from polysilanelike regions, but in high power, high dilution cathode samples containing almost no (SiH₂)_n, nevertheless a peak near 350 °C occurs; (2) the 420 °C peak corresponds to hydrogen released from ≡SiH and/or =SiH₂ sites, both in samples having strong columnar microstructure and in very thin samples—therefore, most likely, near-surface bonded; (3) the peak near 600 °C is related to diffusively delayed evolution of hydrogen from bulk, isolated ≡SiH and/or =SiH₂; and (4) SiH₃ sites, which occur in samples grown at low substrate temperatures, release hydrogen at <250 °C. The latter observation is made in the ir spectra, but is seen in evolution only as a low-temperature tail on the polysilane peak.

Returning to the reported spectra in the literature, we find that we can account for all structure in this unified way. BFZL used samples 0.3–0.5 μm thick, prepared at 25 and 250 °C using 100% SiH₄ at low rf power. The 25 °C, 0.5 μm thick sample had evolution peaks at 350 and 520 °C. These peaks were ascribed to =SiH₂ and ≡SiH, respectively. The 250 °C, 0.3 μm thick sample showed no peak near 300 °C in agreement with the fact that little polysilane should be found in samples grown under the given conditions. The peaks at 400 (weak) and 500 °C (strong), we assume, are due to surface and bulk ≡SiH (or =SiH₂). MMB report work on 300 Å thick films grown at 250 °C using 1% concentration of SiH₄ in argon. Two peaks are observed: one at <300 °C and one at ~385 ±30 °C. The shift to lower temperatures is possibly accounted for by the lower heating rate (12 °C/min). We expect the presence of polysilane in these films (1% SiH₄-Ar), and the very thin samples, allows diffusion to be neglected thus leading

to the low-temperature ≡SiH/=SiH₂ peak.^{15(b)} Of particular note is the observation of H evolution below 150 °C from samples deposited at 250 °C. This demonstrates the existence of short-range motion of hydrogen in films at low temperatures. MP studied 1 μm thick films deposited at 30 and >200 °C. They find peaks at 375 and 600 °C and determined that both evolution peaks correspond to first-order rate processes. Because of the effects of columnar morphology and diffusion, we believe the first-order fit of the high-temperature peak to be fortuitous. (BFZL find their high-temperature peaks to be approximately second order.) TF have measured the changes in ir-mode strengths with annealing. Our mode assignments are in close agreement with theirs, including the 350 °C peak in the evolution rate arising from ≡SiH in cathode samples as noted above.

The origin of the "320 °C" peak is as yet uncertain, but the following tentative explanation is consistent with all observations to date. We start from our assignment of the 420 °C peak to immediate release from isolated ≡SiH/=SiH₂ sites. The various evidence for H motion below 420 °C corroborates the notion that H release must be facilitated by some energy-lowering mechanism. For example, diffusion by bond switching to neighboring sites allows co-release of molecular hydrogen and Si-Si bond reconstruction. Conservation of bond number should lead to a much lower activation energy than a simple one-step atomic hydrogen release. Any microstructure in the sample would probably enhance the likelihood of Si-H/Si-H pairing by effectively reducing the dimensionality of the space of easy diffusive motion. Thus, the presence of microstructure in samples should lower the temperature of maximum release from the 420 °C for homogeneous regions. The fact that samples having columnar morphology always have a 320 °C peak associated with release from (SiH₂)_n and (for thick samples) disintegrate seems to imply that polysilane exists predominantly in the intercolumnar regions. Molecular release and subsequent rapid H₂ diffusion in the intercolumnar regions is indicated. The occurrence of a peak near 350 °C in (the 5%; 25 W; RT; cathode) samples for which no (SiH₂)_n or columnar morphology is observed, may then imply a different microstructural growth pattern. For example, small voids which contain little or no (SiH₂)_n could also enhance the probability of two ≡SiH units becoming neighbors with consequent H₂ release and bond reconstruction.

Before concluding, we discuss the behavior of the luminescence as shown in Figs. 1(c) and 1(d). Although we have found the quenching and shifting of the luminescence band to be similar at low and

high temperatures and to be related simply to the spin density, the origin of the shift in luminescence energy and change in linewidth is in fact different for the two regimes. In the low-temperature regime ($< 250^\circ\text{C}$), the shift to higher energies and narrowing with increasing anneal temperature are quantitatively consistent and accounted for by a reduction in the disorder potential in the band tails. The shift to lower energies at high temperatures with no consequent increase in width is in agreement with the decrease in band-gap when hydrogen is evolved.

IV. CONCLUSION

We infer from the above results the following picture: First, annealing initially reduces the defect density. The mechanism, whether defect motion or hydrogen diffusion, has not been ascertained, but hydrogen release below 150°C tends to

support the latter. The subsequent increase of defect density is dependent *both* upon the nature of hydrogen bonding *and* upon the microstructure and thickness of the samples. The defects annealed out below 250°C and created above, act as nonradiative recombination centers in the same way as found in as-deposited samples—independently of the microscopic origin of the hydrogen evolved. For a given sample, the peaks in the hydrogen evolution do relate to release from specific bonding sites. However, because morphology and diffusion strongly affect the evolution spectra, one cannot, in fact, simply derive binding energies for the various configurations from the spectra.

ACKNOWLEDGMENTS

We wish to thank R. Lujan for his assistance in sample preparation. This work was supported in part by DOE Contract No. 03-79-ET-23033.

¹C. C. Tsai, H. Fritzsche, M. H. Tanielian, P. J. Gaczi, P. D. Persans, and M. A. Vesaghi, in *Proceedings of the Seventh International Conference on Amorphous Liquid Semiconductors*, edited by W. E. Spear (University of Edinburgh, Edinburgh, 1977), p. 339.

²J. I. Pankove and D. E. Carlson, see Ref. 1, p. 402.

³J. C. Knights, G. Lucovsky, and R. J. Nemanich, *Philos. Mag. B* **37**, 467 (1978); M. H. Brodsky, M. Cardona, and J. J. Cuomo, *Phys. Rev. B* **16**, 3556 (1977).

⁴R. A. Street, J. C. Knights, and D. K. Biegelsen, *Phys. Rev. B* **18**, 1880 (1978).

⁵H. Fritzsche, see Ref. 1, p. 3.

⁶M. H. Brodsky, M. A. Frisch, J. F. Ziegler, and W. A. Lanford, *Appl. Phys. Lett.* **30**, 561 (1977).

⁷J. A. McMillan and E. M. Peterson, *J. Appl. Phys.* **50**, 5238 (1979).

⁸C. C. Tsai and H. Fritzsche, *Sol. Energy Mat.* **1**, 29 (1979).

⁹J. C. Knights and R. Lujan, *Appl. Phys. Lett.* **35**, 242 (1979).

¹⁰D. E. Carlson and C. W. Magee, *Appl. Phys. Lett.* **33**, 81 (1978).

¹¹J. Stuke, see Ref. 1, p. 406.

¹²C. Tsang and R. A. Street, *Philos. Mag. B* **37**, 601 (1978); *Phys. Rev. B* **19**, 3027 (1979).

¹³R. A. Street, D. K. Biegelsen, and J. Stuke, *Philos. Mag. B* (to be published).

¹⁴H. Fritzsche, M. Tanielian, C. C. Tsai, and P. Gaczi, *J. Appl. Phys.* **50**, 3366 (1979).

¹⁵(a) K. J. Matysik, C. J. Mogab, and B. G. Bagley, *J. Vac. Sci. Technol.* **15**, 302 (1978); (b) in thicker films, evolution has been found to continue to higher temperatures (private communication).